Published online 28 November 2016

Nucleic Acids Research, 2017, Vol. 45, No. 1 ***255–270***
doi: 10.1093/nar/gkw1148

A genome wide dosage suppressor network reveals genomic robustness

Biranchi Patra[1,†], Yoshiko Kon[2,†], Gitanjali Yadav[1,3], Anthony W. Sevold[1], Jesse P. Frumkin[1], Ravishankar R. Vallabhajosyula[1], Arend Hintze[1], Bjørn Østman[1], Jory Schossau[1], Ashish Bhan[1], Bruz Marzolf[4], Jenna K. Tamashiro[1], Amardeep Kaur[4], Nitin S. Baliga[4], Elizabeth J. Grayhack[2], Christoph Adami[1], David J. Galas[4], Alpan Raval[1,5], Eric M. Phizicky[2] and Animesh Ray[1,6,*]

[1]Keck Graduate Institute, 535 Watson Drive, Claremont, CA 91711, USA, [2]Department of Biochemistry, University of Rochester School of Medicine, Rochester, NY 14627, USA, [3]National Institute of Plant Genome Research (NIPGR), Aruna Asaf Ali Marg, New Delhi 110067, India, [4]Institute for Systems Biology, 1441 N 34th St, Seattle, WA 98103, USA, [5]Institute of Mathematical Sciences, Claremont Graduate University, Claremont, CA 91711, USA and [6]Division of Biology and Biological Engineering, California Institute of Technology, Pasadena, CA 91125, USA

Received July 29, 2016; Revised October 17, 2016; Editorial Decision November 01, 2016; Accepted November 07, 2016

ABSTRACT

Genomic robustness is the extent to which an organism has evolved to withstand the effects of deleterious mutations. We explored the extent of genomic robustness in budding yeast by genome wide dosage suppressor analysis of 53 conditional lethal mutations in cell division cycle and RNA synthesis related genes, revealing 660 suppressor interactions of which 642 are novel. This collection has several distinctive features, including high co-occurrence of mutant-suppressor pairs within protein modules, highly correlated functions between the pairs and higher diversity of functions among the co-suppressors than previously observed. Dosage suppression of essential genes encoding RNA polymerase subunits and chromosome cohesion complex suggests a surprising degree of functional plasticity of macromolecular complexes, and the existence of numerous degenerate pathways for circumventing the effects of potentially lethal mutations. These results imply that organisms and cancer are likely able to exploit the genomic robustness properties, due the persistence of cryptic gene and pathway functions, to generate variation and adapt to selective pressures.

INTRODUCTION

Robustness of biological systems has two different connotations: physiological robustness, which is defined as the ability of an organism to withstand the effects of fluctuations in its environment by maintaining homeostasis (1), and genetic robustness, which is the ability of an organism to withstand the effects of deleterious mutations in its genes (1–3). Genetic robustness leads to physiological robustness through optimization of fitness by competition within an environment (4). Genomic robustness is genetic robustness when applied to the whole set of genes of an organism. In contrast to physiological robustness, which is a property over short time-scales relative to the generation time, genomic robustness is a property of the overall genetic organization of gene sets over evolutionary time scales, or, in the case of cancers, over multiple cell generations. The question of genomic robustness was first experimentally addressed by determining mutational effects on the lysis-lysogny decision circuit of bacteriophage lambda (5). Gene redundancy (6), and promiscuity of gene function (7,8) both contribute to genomic robustness. The core set of essential genes might impede evolvability (9), because any deleterious mutation

*To whom correspondence should be addressed. Tel: +1 909 607 9729; Email: aray@kgi.edu
Present addresses:
Ravishankar R. Vallabhajosyula, Impetus Technologies, Los Gatos, CA 95032, USA.
Alpan Raval, Institute of Mathematical Sciences, Claremont Graduate University, Claremont, CA 91711, USA.
Jory Schossau, Computer Science and Engineering, Michigan State University East Lansing, MI 48823, USA.
Arend Hintze, and Christoph Adami, Microbiology and Molecular Genetics, and BEACON Center for the Study of Evolution in Action, Michigan State University, East Lansing, MI 48823, USA.
Bjørn Østman, Ecology, Evolution, and Marine Biology, University of California Santa Barbara, Santa Barbara, CA 93106, USA.
David J. Galas, Pacific Northwest Diabetes Research Institute, 720 Broadway Seattle, WA 98122, USA.
†These authors contributed equally to the paper as first authors.

in these genes would reduce fitness. However, epistasis and modular rewiring of genetic networks may in principle overcome this barrier (2,10). Biological interaction networks are robust to perturbation (1,11–14) because of several features, including power-law network topology, redundancy, modularity and their dynamic properties (1,3,15–25). Recent studies have revealed dynamic interaction among apparently unrelated gene modules in response to genotoxic stress, suggesting the existence of highly reconfigurable networks of gene and protein modules as well as of unexpectedly plastic macromolecular complexes (26,27). Although modularity is a common feature of interaction networks, which is thought to contribute to physiological robustness (20,26,28–31), the contribution of modularity to genomic robustness is difficult to determine (16).

The suppression of essential gene mutations has been classically employed to investigate gene function, and suppressors provide clues to mechanisms of evolution (8,32–33). Here we use genome wide dosage suppressor (DS) analysis to probe mutational robustness of the genome. As opposed to secondary mutations that cause survival in the presence of deleterious primary mutations, here we artificially enhance the expression of nearly every gene in the genome to determine which of these (i.e. DSs) could allow survival secondarily in the presence of a deleterious primary mutation. We tested the hypothesis that the network of DS genes is modular. To probe molecular mechanisms of robustness, we focused on a small set of essential genes related to vital cellular processes, such as DNA replication, cell cycle control, RNA synthesis and processing. We have uncovered 660 pairs of DS-mutant gene interactions (out of a theoretical maximum of 27401 interaction pairs) involving 517 suppressor genes and 53 mutant alleles. We report the discovery of at least one novel mechanism of robustness in a eukaryote, namely, the engagement of promiscuous gene functions through degenerate pathways.

MATERIALS AND METHODS

MORF plasmids

The movable open reading frame (MORF) library (34) containing 5871 2μ plasmids with galactose inducible promoter and a *URA3* selectable marker were divided into 16 pools. Each pool, representing approximately 384 plasmids, was grown in 96 deep-well plates, pooled, and plasmid DNA samples were isolated for transformation.

Yeast strains, media and transformation

Temperature sensitive lethal *Saccharomyces cerevisiae* strains had specific mutations in BY4741 background (*MATa his3Δ1 leu2Δ met15Δ ura3Δ*); point mutants were provided by Dr Charlie Boone (University of Toronto) (35) and *ts* deletion mutants were screened and selected from the deletion mutant library (OpenBiosystem). Note that yeast temperature sensitive lethal mutant alleles are often combinations of multiple base changes in the same gene, but for the purpose of this work we consider such combined lesions as one allele. For each mutant, the range of growth and the threshold of non-permissive temperature on both inducing (+galactose) and non-inducing (−galactose) conditions were determined. Yeast strains were grown in yeast complete media containing 1% raffinose, transformed with 1 μg of each MORF plasmid pool and plated at permissive temperature on synthetic defined medium lacking uracil with 1% raffinose. The transformants from 16 plates were pooled and selected at the restrictive temperature for that particular *ts* allele on complete and synthetic media containing either 2% glucose (repression) or 2% galactose (induction) (see Supplementary Table S1A) for a list of restrictive temperatures corresponding to the *ts* alleles). The threshold restrictive temperature that cuts off the growth of each individual allele with or without (vector control) the candidate suppressor plasmid was determined for each suppressor by incubating identical multiple-replicate plates at a range of temperatures spanning at least ±2°C around the restrictive temperature for that allele. Transformants in each mutant strain were selected for growth above the respective restrictive temperature characteristic for the corresponding mutant strain containing the empty vector plasmid.

Suppressor identification and confirmation

Suppressor MORFs were identified and confirmed by 3-fold cross validation as described below. Candidate hits were first identified by microarray hybridization of isolated plasmid DNA from colonies growing above the restrictive temperature for the respective *ts* allele as follows: ∼300 colonies were picked from selection plates at restrictive temperature, grown in 96 deep-well plates. The cells were pooled and plasmid DNA isolated using Cycle Pure Kit from Omega Bio-Tek and labeled with Cy3 dye, whereas the pooled DNA of the MORF library was labeled with Cy5 by polymerase chain reaction (PCR) amplification using two flanking primers (5'GGACCTTGAAAAAGAACTTC3', 5'CCTCTATACTTTAACGTCAAGG3'). Labeled probes were hybridized to spotted microarrays (UHN Microarray; containing >95% of all open reading frames (ORFs)) at 65°C for 16 h. Microarrays were scanned in Bio-Rad VersArray Chip Reader and the data were analyzed using ScanArray express software 3.0 (Perkin Elmer). Second, once candidate suppressors were identified by microarray hybridization the suppressor genes were subsequently PCR amplified from the individual MORF DNA from the single colonies that generated the pools, and were analyzed by agarose gel electrophoresis for the expected size bands for the corresponding gene; where there were discrepancies, the candidates were discarded. Approximately 70% of the hits could be validated at this step. Third, with all remaining candidates that exhibited the correct gene size by PCR, the corresponding plasmid DNA from the MORF library (not from the candidate colonies) were reintroduced into the corresponding yeast mutant strain and tested again for suppression to confirm the candidate gene. Over 95% of candidate genes could be validated at this stage. For a limited number of suppressors (130), we purified the DNA from colonies growing on selection plates with raffinose and galactose, transformed into *Escherichia coli*, re-isolated the corresponding plasmid DNA samples, PCR amplified the ORF off the MORF plasmids and sequenced the DNA. In all cases, the suppressor MORFs identified by sequencing

were identical to the MORFs identified by microarray hybridization, and no mutation was ever detected within the sequenced regions. The putative suppressor genes identified by either microarray or by direct sequencing were retransformed individually to the respective mutant strains, their ability to suppress the mutants confirmed individually on at least three separate transformed colonies by isolating single colonies and testing on inducing or non-inducing plates at a range of temperatures above the growth cutoff temperature of the corresponding unsuppressed mutant, dependence of suppression on the introduced MORF plasmid was confirmed for each transformant on plates containing 5-fluroorotic acid and for those transformants passing all above tests the titration-spotting test was carried out for final confirmation/quantification of suppressor strength. The background strain was always compared on the same plate with the candidate-suppressed strains at a range of temperatures spanning at least 1°C over the corresponding threshold temperature for growth of the given mutant. The extent of suppression was subsequently quantified through spotting of serial dilutions of each mutant/suppressor culture under both inducing and non-inducing conditions. A subset of the final list of suppressors was again confirmed by sequencing. The negative control for each suppressor was the corresponding mutant strain carrying the empty MORF vector (BG1776). Positive control plasmids were the complementing genes under pGAL control, except for six mutants (*cdc13, cdc4, cdc15, cdc35, cdc48* and *abd1*) that did not have the appropriate positive controls because either the over-expression of the corresponding MORF plasmids was lethal (*CDC13* and *CDC48*) or they were absent in the MORF library (*CDC4*, *CDC15*, *CDC35* and *ABD1*). The strength of suppression for each suppressor was normalized to the growth of the diluted spots against that of the corresponding vector control (BG1776) strain on the same plate on adjacent rows (Supplementary Table S2). Finally, to address the concern that some of the MORF plasmids in the library might be mislabeled, we picked at random 85 MORF DNA samples from the collection of 517 non-redundant suppressor MORFs and sequenced them. All 85 sequences out of 85 confirmed the correct MORF. Therefore, the chance of an error due to MORF mislabeling in the full dataset (assuming the errors are randomly distributed with a small mean), by Poisson distribution, is at most $(1–e^{-1/86}) = 0.012$, or at most 6 among 517 suppressors.

Protein detection

Cultures were grown in repressing and inducing media, and whole cell extracts were prepared by the bead beating method in yeast lysis buffer (25 mM Hepes-NaOH pH 7.5, 10 mM NaCl, 1 mM ethylenediaminetetraacetic acid (EDTA), 0.1% Triton X-100) containing EDTA–free complete protease inhibitor tablet (Roche). Proteins were detected by Western Blotting, probed by anti-HA antibodies (Covance) using standard methods.

Liquid growth assay

Growth curves in liquid media along with maximal growth rates were determined using a Bioscreen C Automated Growth Curves Analysis System (Growth Curves USA). The suppressed strains were grown in 200 μl of S-URA with 1% raffinose and 2% galactose at various temperatures in 96-well plates. The optical density (OD) was measured at 600 nm every 30 min for 48 h of growth.

RNA methods

Strains were grown in 5 ml S-URA media containing 2% raffinose for 24 h at 28°C. Samples were diluted to OD 0.02 in 150 ml S-URA media containing 2% raffinose and 2% galactose and then grown overnight at 25°C with agitation. At OD 0.1, cultures were shifted to 34.5°C with continuous agitation and samples were harvested at 0, 45, 90 and 180 min by centrifugation. Total RNA was isolated using a hot phenol method (36), followed by two chloroform extractions, RNA precipitated by addition of 1/10th volume of NaOAc pH 5.2 and 2.5 volumes of 100% ethanol and the pellet dissolved in 50 μl ddH_2O. Total RNA was deproteinized again after DNase treatment and resuspended in 10 μl of ddH_2O, and quantified by a nanodrop spectrophotometer.

Gene expression measurements

One microgram total RNA samples from two individual biological replicates, four time points each (0, 45, 90 and 180 min), of *smc2-8* mutant strains harboring pGAL:SMC2, pGAL:UME1, pGAL:MEK1, pGAL:HTA2, pGAL:SNU66 and the negative control MORF plasmid (pGAL:negative, BG1766), were reverse transcribed, hybridized to Affymetrix Yeast Genome S98 arrays and scanned with Affymetrix GeneChip Scanner 3000. The microarray data were analyzed with GeneSpring 6.2 software, and were deposited in Gene Expression Omnibus (accession number GSE24266). Microarray expression levels were verified for seven reference genes by quantitative RT-PCR using samples of a third biological replicate (Supplementary Figure S7).

Microarray data analysis

The Affymetrix array data were processed using the robust multi-array analysis as described previously (37). A log scale, linear additive model represented the perfect match and mismatch data. For each experiment (time point or condition), the RMA analysis produced one numerical estimate of expression for every probe on the chip (two replicates for each treatment and time point). We combined the replicates using a median based normalization (given microarray replicates 1 and 2, determined the median intensities m_1 and m_2 of microarray 1 and microarray 2 respectively; adjusted the values of microarray 2 by adding $m_1–m_2$ to the intensities of microarray 2) to produce an average of the adjusted intensities. For each time point and treatment we produced one intensity measurement for each probe. These numbers were used to find ratios of fold change from one time point to the next. For each chip, a background noise intensity measure was formed using the average intensity of the SPACER probes which act as a set of negative controls for the chip—if for a particular probe, the intensity level at

time points t_1 and t_2 was below the background noise level at t_1 and t_2, then we assumed the probe was expressing at background noise level and the fold change was set to 1. We clustered genes that were significantly differentially expressed in at least one time point.

Quantitative RT-PCR

DNase treated RNA was reverse transcribed in 25 μ_l RT reaction mixtures (1× First Strand Buffer, 0.02 μg random hexamers, 0.01 M DTT, 0.5 mM dNTP mix, 0.6 U RNaseOUT, containing 3 U Superscript II Reverse Transcriptase) for 2 h at 37 °C, followed by heat inactivation at 100°C for 5 min and quick chilling on ice. A standard curve was generated for each gene target starting with 0.5 μg RNA and four successive 2-fold serial dilutions. The cDNA templates generated by reverse transcription was used for quantitative RT-PCR in Applied Biosystems 7500 FAST Real Time PCR system. The PCR mix constitutes 20 μl buffer containing 1× FAST SYBR Green Master Mix and 0.2 μM forward and reverse primers (IDT), with the PCR conditions: [95°C → 20 s] HOLD, [95°C 3 s → 60°C 30 s] 40 times). The following primers were used for real time PCR of seven genes:

Table: Listof Primers for Real Time Quantitative PCR

OPT2 Forward Primer	GGG CTT TGA ATT TGT GGG CCA TGA
OPT2 Reverse Primer	TCA TAA TCG TCG AGC GCC CTG TAA
SMC2 Forward Primer	AAC TTG TGC CGG AGG TAG GCT ATT
SMC2 Reverse Primer	GCC AAT TCA ACT TTC CCA GGA GCA
PHO5 Forward Primer	AGA CAT GCT CGT GAC TTC TTG GCT
PHO5 Reverse Primer	AAG CAC TCA AAG TGT TGG CAC CAG
CYC7 Forward Primer	AGT ACG GGA TTC AAA CCA GGC TCT
CYC7 Reverse Primer	GTC CAA CTT TGT TAG GAC CAC CCT
GRE1 Forward Primer	ACT GGT GGT GGC ACT TAT ACC CAA
GRE1 Reverse Primer	TGG TAG CGG TTA CTT TGA GCA CCT
SIP18 Forward Primer	AGG GAA AGA ACG CCA AAT CCT CCA
SIP18 Reverse Primer	CAA TCG TTC GCA ATT CCT CTG CCA
FIT1 Forward Primer	TGC CCA ATC TGT TCG TAC CCA TGA
FIT1 Reverse Primer	ACC AGC GGT AGT GGT TTG AAC TCT

Datasets

The full DS dataset (DS-ABC, see text), consisting of data reported here combined with other available data, was culled from the following sources: Magtanong *et al.* (33), the latest BioGRID version 3.1.78 (38) and this work (660 DS interactions between 53 mutant ORFs and 517 suppressor ORFs). The full DS dataset contains 2286 interactions between 454 mutant ORFs and 1284 suppressor ORFs, and includes 60 reciprocal interactions, resulting in 2226 unique interactions (see Supplementary Table S6). The protein–protein interaction (PPI) network was constructed from BioGRID version 3.1.78 (38) that contains 6614 ORFs of which 5955 nodes are connected by physical interaction edges. The 99 866 physical interactions produced 60 143 unique edges among 5728 nodes. This network was curated to filter out indirect physical interactions and retain only the direct physical interaction data from eight types of experiments including Biochemical activity, co-crystal structures and reconstituted complexes, co-immunoprecipitation, protein–peptide interactions, two-hybrid, far western and FRET. The resulting direct PPI network, containing a total of 20034 unique interactions between 4683 nodes (Supplementary Table S14), was used for studying the enrichment of PPI interactions in the DS network. Genetic interaction (GI) data were downloaded using the latest BioGRID version 3.1.78 (38), which contains eleven kinds of GIs, namely, Dosage growth defect, Lethality, Dosage Rescue, Negative Genetic, Phenotypic Enhancement, Phenotypic Suppression, Positive Genetic, Synthetic Growth Defect, Synthetic Haplo-insufficiency, Synthetic Lethality and Synthetic Rescue. In all, the GI dataset includes 16898 interactions between 5411 nodes. The Stanford Microarray Database was used for inferring co-expression between yeast ORFs at a correlation coefficient cut-off of ±0.5. The resultant co-expression network includes 623224 unique edges between 5155 nodes from total 643 experiments reported by two groups (39,40). Genome-wide protein complex data was inferred by combining the Curated Yeast Complexes (CYC2008), a comprehensive catalog of manually curated 408 heteromeric protein complexes in *S. cerevisiae* with 400 complexes in the annotated yeast high-throughput complexes derived from high-throughput Tandem Affinity Purification/Mass Spectrometry (TAP/MS) studies (41), and 72016 pairs of indirect physical interactions from Affinity Capture, Co-Fractionation, Co-purification and Co-localization experiments (BioGRID version 3.1.78). The Pfam domains for many yeast proteins have been assigned one of four age groups ABE, AE/BE, E and F depending on their taxonomic distribution among archaea (A), bacteria (B), eukaryote (E) and fungi (F) (42). This dataset was used to analyze whether DS pairs were likely to belong to the same age group. Both the DS datasets were tested for significant overlap with computationally predicted modules. For this, 41 Yeast Louvain modules were identified in the Yeast direct PPI network by using the NetCarto algorithm (43). In addition, Markovian clusters were identified using the MCL-MLR clustering method (44) at an inflation value of 2.4. Statistical tests are described in Supplementary Data. The frequency distribution of suppressors of strength ≥3 on a per gene basis was not significantly different from the frequency distribution of suppressors of all strengths ($P \sim 1.0$) (Supplementary Table S15 and Figure S3). Therefore we did not separately parse the suppressors by their respective suppression strengths in our analyses.

Paralog identification

The list of paralogs (554 gene pairs) was described before (45), and includes 457 pairs previously found (46). Of the 1108 paralogous genes, 1001 were represented in the MORF library. To test for significant enrichment of paralogs, we performed a Fisher's exact test using the 5829 testable ORFs as the baseline.

Network properties

Betweenness centrality (BC) (fraction of shortest paths through a node) was $B_i' = \sum_{\text{all pairs}} b_i$, where b_i is the ratio of the number of shortest paths between a pair of nodes in the network that pass through node i. BC was scaled as $B_i = \frac{2B'_i}{(n-1)(n-2)}$, where n is the number of nodes in the network (47). Clustering coefficient (ratio of the actual number of degrees of a node to the possible degrees given a node's

neighbors), and shortest path between pairs were computed using the MATLAB Boost Graph Library toolset.

Functional congruence assessment

Functional gene annotations were derived from the MIPS FunCat database (48). A total of 449 of the 642 unique suppressors were annotated genes. Un-annotated genes (class '99') were excluded. Here, functional congruence between two genes is defined as the extent of overlap between their respective MIPS annotations. Because MIPS functional annotations are hierarchical categories, we studied the congruence of MIPS annotations based on the first category alone, first and second, first, second and third, etc. categories, down to congruence in all five categories. Because genes can have several MIPS annotations, we compiled the possible pairs of categories for each pair of genes and calculated the fraction of pairs of annotations that agreed, divided by the number of possible pairs of annotations. Because many annotations do not include details up to the fifth functional categorization, we devised rules to match annotation strings of different length. For example, when matching the functional MIPS annotation '01.01.05.01.02' (degradation of polyamines) with '01.01.06' (metabolism of the aspartate family), we pad annotations such that the previous example would result in a match at level 1, a match at level 2, but not at level 3 and beyond. In other words, for incomplete annotation the omitted part is assumed to be different from that of any other annotations. The functional congruence of two genes at level n is the fraction of annotations of these genes that are identical up to level n. By design, the functional congruence of a pair at level n is larger or equal to the functional congruence of that pair at level $n+1$.

RESULTS

A genome-wide screen for dosage suppressors

We transformed 108 isogenic yeast strains each containing a temperature sensitive (*ts*) point mutation (85 mutants) (35) or a *ts* deletion mutation (23 mutants) (49) with pools of the entire MORF library plasmids ('Materials and Methods' section, Supplementary Table S1A). The use of this library permits interrogating every conditional mutant with virtually every yeast ORF, under conditions where each ORF is expressed in the presence of galactose or glucose (Figure 1A–C). The mutant genes were chosen mostly on the basis of their known functions related to RNA polymerase/RNA modification and/or cell cycle/DNA replication. We transformed each mutant strain with high copy 2μ based plasmids expressing ORFs under pGAL promoter control (34), selected the transformants at the permissive temperature (25°C), then tested for the ability of the recombinant plasmids to rescue growth defect above the specific restrictive temperature for the corresponding mutant strain (see 'Materials and Methods' section). Each candidate suppressor ORF, identified first by hybridizing purified plasmid DNA from candidate suppressed strains on DNA microarrays, was individually confirmed by multiple retransformation and validation experiments and a randomly chosen subset (~130 MORF plasmids re-isolated from suppressed strains) by sequencing (see 'Materials and Methods' section for details). We obtained 660 confirmed DS interactions for 53 of the 108 *ts* mutants that we tested (Figure 1C and Supplementary Table S2). These 660 interactions involved 517 suppressor genes, all of which were individually confirmed through retransformation and repeats of the assays. We confirmed all suppressors of a third of the mutant strains collection independently twice at two different sites (University of Rochester and Keck Graduate Institute). A total of 642 out of 660 interactions are novel; 18 were reported earlier. These results did not find 147 multicopy suppressor interactions previously reported in the literature corresponding to the 53 query mutants (Supplementary Table S3). We directly tested 57 of these previously reported suppressor interactions (corresponding to seven query mutant genes), chosen arbitrarily from among the 147 interactions. We were able to confirm by our methods 15/57 interactions (Supplementary Table S4). As expected, strain background, allele differences, copy number of the plasmids, promoters used for gene expression and/or the levels of galactose-induced gene expression (including leaky expression in the absence of galactose) are sufficiently different among these studies, such that a direct comparison is not possible. Therefore, each case of confirmed suppression should be considered as a suppression event that is true under at least one set of conditions. In certain selected examples of weak suppression, we have noted improved suppression when the suppressor gene is expressed under a constitutive promoter (pTEF1) as compared to that with galactose induced promoter (data not shown).

The DS gene set is enriched for gene ontology (GO) molecular functions (See Supplementary Table S5, and description of significance calculation methods in Supplementary Data), transcription factor activity (Benjamini-Hochberg corrected enrichment significance $P = 9 \times 10^{-35}$) and ribosome structural components (Benjamini-Hochberg corrected enrichment significance $P = 4 \times 10^{-4}$). A fuller description of the functional implications of this set of suppressors is provided in later sections.

Computational analysis reveals uniqueness of dosage suppressor networks

In this and the following sections we explore general properties that might distinguish this large dataset of DSs of gene mutations from those reported previously.

The DS network discovered here (dataset DS-A, Supplementary Table S6), containing 53 *ts* mutants and 517 suppressor genes, exhibits a large connected component (560 nodes, 656 edges) (Supplementary Figure S2) that excludes 29 unconnected nodes and 20 edges. Of the 517 suppressor genes, 134 are of unknown function at the time of writing. Previous work (33) had examined the entire collection of DSs of essential gene mutants known at the time that included those reported in BioGrid (dataset DS-B; Supplementary Table S6B) and 214 suppressor genes they discovered for 29 mutants (dataset DS-C; Supplementary Table S6C). All three datasets together (DS-ABC; Supplementary Table S6D) comprises 2286 dosage-suppressor interactions (Supplementary Figure S3).

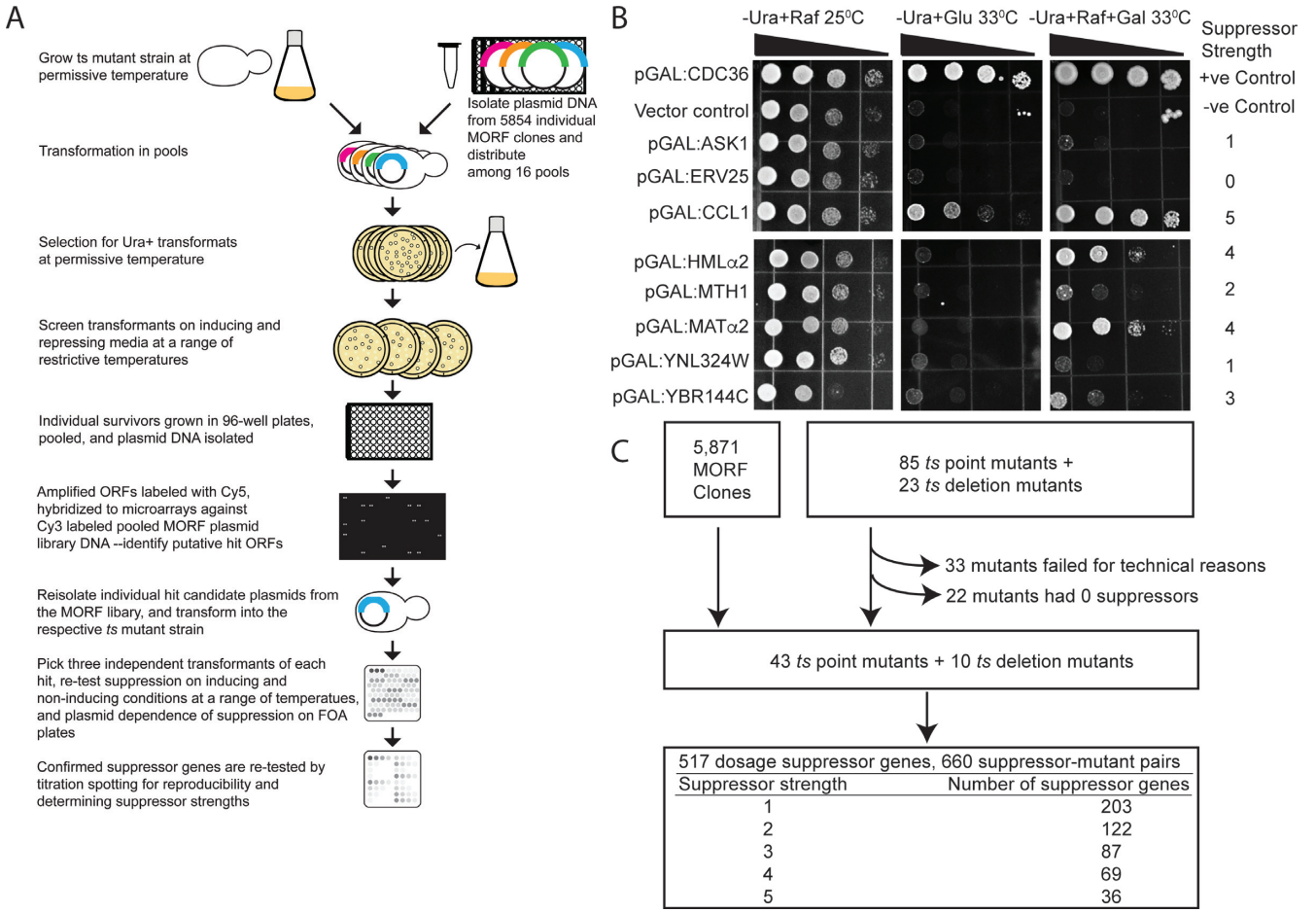

Figure 1. Systematic discovery of dosage suppressor (DS) genes. (**A**) The strategy for isolating DSs of *ts* lethal mutations. See 'Materials and Methods' section for details. (**B**) A few examples of suppressors of different strengths. A *ts* allele of *cdc36* is viable at 25°C, but fails to grow above 33°C, is complemented by pGAL:CDC36 at 35°C or below under all tested conditions (galactose independent) and is suppressed by *MATα2* (strong, grade 4), *MTH1* (medium-weak, grade 2), *CCL1* (strong, grade 5) and *ASF2* (strong, grade 5). The latter two genes exhibit galactose independent suppression. Galactose-independent suppression generally implies leaky expression of the ORF through the pGAL promoter on a multicopy plasmid even in the absence of galactose. This is consistent with expression of the corresponding protein in the absence of galactose, as determined by western blots (see Supplementary Figure S1 for an example). YNL324W is a very weak suppressor (grade 1, but reproducible). pGAL-negative is the vector control. (**C**) Summary of the screen. Most suppressors were effective on galactose but not on glucose (Supplementary Table S2); a few exceptional suppressors are galactose independent (see above), presumably because these expressed detectable quantities of MORF-encoded protein on western blots even on glucose (see Supplementary Figure S1 for examples). The 22 mutants (Supplementary Table S1B) that failed to yield suppressors did however yield the wild-type complementing ORFs.

Paralogous genes do not explain most suppression mechanisms

Gene redundancy is one of the ways robustness might be encoded within the genome. The redundancy of genes leads inevitably to divergence by mutational pressure, and we recognize ancestral gene redundancy by the presence of paralogous gens, where gene pairs are structurally and functionally similar but nonidentical. We addressed whether suppression by paralogous genes could potentially explain mechanisms of suppression. Suppressors in DS-A are not significantly enriched (Fisher's exact $P = 0.65$) for paralogs: only 93 out of 517 genes in the suppressor network have at least one known paralog, as determined by the curated list of 'ohnologs' (paralogs descended from whole genome duplication events) (45). Among the 93 paralogs, we found 20 paralogous partners within mutant-suppressor sets (Table 1). Seven out of ten paralogous partners encode ribosomal proteins, where each paralog suppresses the same mutation. Not all ribosomal protein genes suppressed the same mutations, and some ribosomal protein genes suppressed multiple mutations (Supplementary Table S7). These results suggest that additional mechanisms, such as suppression through PPI or through gene network rewiring, must be involved in most instances of dosage suppression discovered here.

Analysis of Co-suppressor networks

If paralogous genes cannot explain most suppression mechanisms, is there evidence that the co-suppressors might be enriched for remnants of conserved functions over evolution? Therefore, we examined functional similarity among the genes discovered through this study with those in previous studies in three different ways.

Table 1. Paralogous pairs of dosage suppressors

Paralog 1	Gene name	Mutation(s) suppressed by paralog 1	Paralog 2	Gene name	Mutation(s) suppressed by paralog 2
YBR181C	*PRS6B**	*cdc24, cdc15*	YPL090C	*RPS6A**	*cdc24, cdc15, poc4*
YCR073W-A	*SOL2*	*cdc26*	YNR034W	*SOL1*	*cdc26*
YDR099W	*BMH2**	*cdc25*	YER177W	*BMH1**	*cdc25*
YDR471W	*RPL27B**	*pol5*	YHR010W	*RPL27A**	*pol5, cdc25*
YER056C-A	*RPL34A**	*cdc48*	YIL052C	*RPL34B**	*cdc48*
YER131W	*RPS26B**	*vrp1*	YGL189C	*RPL26A**	*vrp1*
YFR023W	*PES4*	*smc2*	YHR015W	*MIP6*	*smc2*
YJL177W	*RPL17B**	*cdc48*	YKL180W	*RPL17A**	*cdc48, cdc13*
YLL062C	*MHT1*	*taf14*	YPL273W	*SAM4*	*taf14, cdc13*
YLR029C	*RPL15A**	*cdc24, cdc26*	YMR121C	*RPL15B**	*cdc24*

*Ribosomal genes.

First, are DS genes and their corresponding suppressed mutant genes functionally related? A total of 20 out of 660 mutant-suppressor pairs in DS-A shared the same gold standard GO (50) terms (binomial $P < 10^{-15}$), and 922 of 2286 known mutant-suppressor pairs (in DS-ABC) shared the same GO gold terms (binomial $P < 10^{-15}$) (Supplementary Table S8).

Second, if the mutant genes and their suppressors are functionally related, then they should be enriched for GIs. To test, we intersected the DS-mutant gene pairs with known GI pairs (51) and found significant enrichment ($P = 5.34 \times 10^{-8}$) for 11 kinds of GIs (51) (Supplementary Table S9). For 30 of the 660 gene pairs in DS-A (∼4.5%), a previously reported GI was found to exist (see Supplementary Table S9 for details). A large fraction (547/660), however, was not found to overlap with known physical or GI pairs.

Third, we mapped the genes of each of the three networks (DS-A, DS-B and DS-C) on to a curated and integrated PPI network (28,52–55) (see 'Materials and Methods' section for the integrated PPI dataset). We determined functional similarity between proteins encoded by these genes, by comparing their MIPS (Munich Information Center for Protein Sequences) functional catalog annotations (48). Functional similarity, defined by the functional congruence (see 'Materials and Methods' section) of a *ts*-mutant gene with its suppressors, is significantly lower than that which would be expected for proteins having a direct physical interaction (Wilcoxon rank-sum $P = 2.26 \times 10^{-14}$) (Supplementary Figure S4A). As a comparison, the functional congruence between a *ts*-mutant and its suppressors is also lower for DS-C network than that for DS-B, whereas that of DS-B is comparable to that in the curated PPI network (Supplementary Figure S4A). These observations suggest that DS-A and DS-C reveal suppressors that are qualitatively different from those revealed by the focused methods used by earlier workers, which predominate in DS-B. The functional congruence among co-suppressors of the same mutant in DS-A is comparable with the congruence between proteins that share a physical edge in the curated PPI network (Supplementary Figure S4B). However, the co-suppressors of the same mutant for DS-A are considerably more diverse than those in DS-B or DS-C (Supplementary Figure S4B), once again demonstrating a distinct collection of dosage-suppressors discovered here.

To further examine the uniqueness of the dosage suppression network discovered here, we calculated topological properties of the corresponding protein nodes in the PPI networks described above (Supplementary Table S10). DS-A comprising 660 interactions overlapped significantly with the PPI network ($P = 2.8 \times 10^{-15}$, see Table 2). The previous dosage-suppressor collection (DS-B and DS-C) also showed a statistically significant overlap with the curated PPI. The degree and clustering coefficient of the DS gene nodes in the PPI network are not significantly different among the three DS datasets. By contrast, the values of another topological property, BC (see 'Materials and Methods' section for definition) of the nodes in DS-A or DS-C are significantly higher than the nodes in DS-B (Supplementary Table S10). A statistically significant overlap with PPI network implies that the mutant-suppressor pairs may belong to the same protein modules or complexes. We next explicitly examine this question.

Modular organization of interacting proteins can explain suppression mechanisms

Most suppression mechanisms cannot be ascribed to the functions of individual genes/proteins in the absence of targeted genetic or biochemical studies. However, it should still be possible to derive general principles by examining the existence of functional modules in the DS network. Biological networks have underlying modular sub-structures that reflect functional organization and evolutionary origins of gene products (56,57). Because there is no unambiguous definition of a module within protein networks, we examined three intrinsically different concepts of modularity. First, we examined the enrichment significance of protein products of the suppressor interaction network within the protein complexes that are manually curated clusters obtained from physical PPI data (41), by determining the overlap of proteins of the 660 mutant-suppressor pairs with these complexes (41,38) (see Supplementary Data for a discussion of how the overlap is measured and Supplementary Table S9 for overlap significance *P*-values). The products of each member of 54 pairs of the total 660 dosage-suppressor pairs were found within the same protein interaction complexes (binomial $P < 10^{-15}$) (Table 2) (binomial test is an exact test for estimating deviations from a theoretical distribution separable into two categories, which is the appropriate

Table 2. Similarities between mutant genes and their suppressors

Number of mutant-suppressor gene pairs	Among dosage suppressor pairs (total 660) discovered in this work		Among all known dosage suppressor pairs (total, 2286)	
	Number	Enrichment significance (Binomial one-sided test *P*)	Number	Enrichment significance (Binomial one-sided test *P*)
With direct PPI	23	2.5×10^{-14}	445	$<10^{-15}$
Co-located in the same protein complex	54	$<10^{-15}$	558	$< 10^{-15}$
Co-located in the same computationally predicted protein module[#]	71	1.3×10^{-5}	557	$<10^{-15}$
Co-located within the same PPI cluster[##]	12	2.04×10^{-5}	232	$<10^{-15}$
In which both genes are co-expressed	10	0.263097*	144	3.1×10^{-12}
In which both genes are of similar evolutionary age	159	0.06422174*	641	1.8×10^{-10}

*No statistically significant enrichment.
[#]Co-located in one of 41 Louvain modules, computed by the Netcarto algorithm (43).
[##]Co-located in Markovian clusters, computed by MCL-MLR clustering (44).

condition here). When the entire collection of 2286 dosage-suppressor pairs known so far (DS-ABC dataset) was so examined, 558 pairs co-occur in the same protein complexes (binomial $P < 10^{-15}$), signifying that in the full dataset also mutant genes and suppressor genes tend to express proteins that belong to the same complexes. These results suggest that the suppressors and their respective suppressed genes define modular elements within protein–protein complexes.

To directly determine whether the suppressor dataset is modular, protein modules were obtained by computationally optimizing a modularity measure on the PPI network (43), then the overlap of the proteins of the mutant-suppressor pairs within these computationally determined protein modules. Similar associations as with the first approach were observed within the computationally predicted PPI clusters (Supplementary Table S9). Using a yet another concept of modularity, we identified modules dynamically, by sequentially removing genes from a curated PPI network constructed from the DS pairs (see 'Materials and Methods' section), starting with the highest betweenness central (BC) gene and re-computing the BC of nodes in each resulting network, leading to a measure of modularity (58). BC of a node (i.e. a gene, for our purposes) is the ratio of the number of shortest paths between a pair of nodes, which passes through that node, to the total number of shortest paths that pass through that node. If one ranks gene by their BC values, and systematically remove them from the highest BC down, then the network becomes progressively unconnected. However, if the network is modular then the rate at which the network gets unconnected is slower than if the network is not modular: this is because the high BC nodes generally occur between strongly connected (or modular) node sets. Thus, gene pairs that predominantly lie within modules should remain connected in the PPI network longer than the average pair, while gene pairs that straddle modules should separate earlier. We find that throughout this iterative process the mutant-suppressor pairs in the dataset DS-A were more likely to be found within module boundaries (Wilcoxon rank-sum $P = 2.26 \times 10^{-14}$; Supplementary Figure S5) (Wilcoxon rank-sum is a nonparametric hypothesis test appropriate for comparing a pair of matched samples) than were the randomly chosen protein pairs, than were the pairs in dataset DS-C (33) ($P = 1.55 \times 10^{-13}$) or than were those in the dataset DS-B ($P = 2.14 \times 10^{-10}$). That the mutant-suppressor pairs lie preferentially within module boundaries is consistent with the observed distribution of mutant-suppressor distances within the PPI network (number of edges along the shortest path in the PPI network connecting the mutant to the suppressor; see inset in Supplementary Figure S5).

Modularity of the suppressor dataset allows a method for exploring the functional organization of genes and their products. As a first step in such a process, we determined the identity of the complexes within which the mutant-suppressor pairs co-occurred. By culling from the BioGRID database 4632 direct PPIs and by identifying protein clusters using simulated annealing (43), we generated 41 modules (Supplementary Table S11). We queried each mutant-suppressor pair discovered in DS-A for their co-occurrence in these 41 modules, and found eight such modules containing five clusters and three singletons (Figure 2). One module (Figure 2A) shows that mutations in cell cycle control genes *cdc28* (a CDK), *cdc20* and *cdc16* (both anaphase promoting complex protein genes) and *cdc37* (encodes an HSP90 co-chaperone), are suppressed by several genes including a ribosomal protein gene *MRPL50,* and *MPD1* that encodes an endoplasmic reticulum chaperone interacting protein, underscoring the importance of molecular chaperones and ribosomal proteins in facilitating the suppression of point mutant alleles. In a second module (Figure 2B), mutations in *cdc9* (DNA ligase), *tfb3* (transcription coupled DNA repair) and *pob3* (encodes a member of the FACT complex for nucleosome reorganization) are in the same module with several suppressors including *PSY3* (DNA repair-recombination), and *SSL2* (DNA repair helicase), suggesting the possible involvement of these proteins for overcoming DNA damage/repair defects. A third module (Figure 2C) contains two suppressors of *SEC18* and *TEM1*, one of which has no known function. As expected, well known multi-protein complexes, including the RNA–PolII complex (Figure 2D) and the DNA condensin–cohesin complex (Figure 2E) could be recovered.

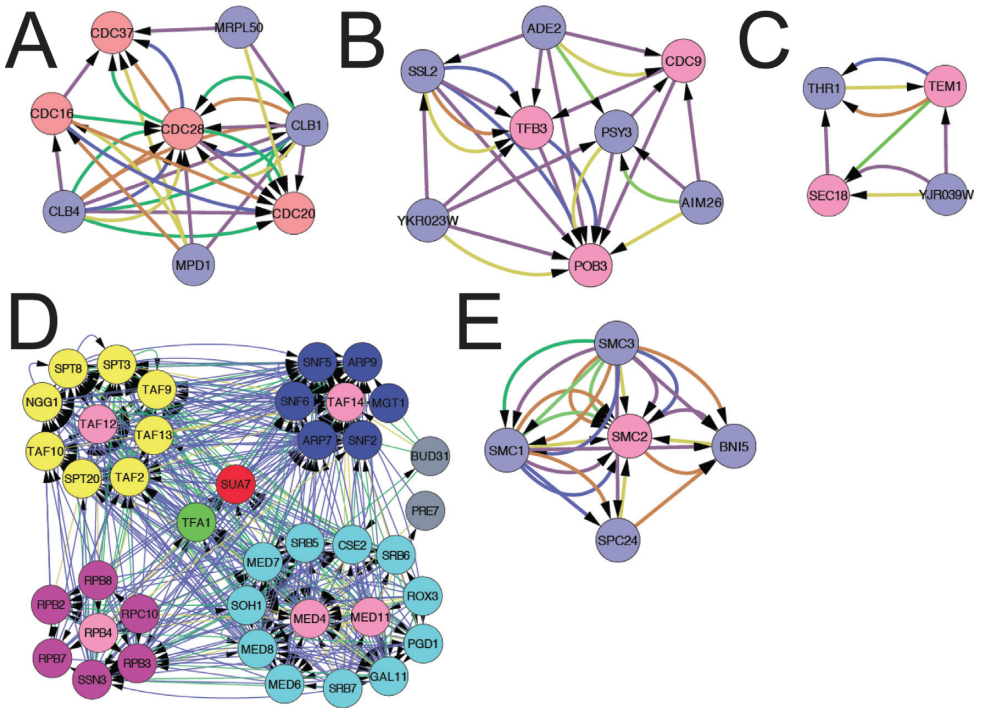

Figure 2. Mutant-suppressor pairs are enriched within protein modules. Five computationally predicted modules in which specific mutant-suppressor pairs are statistically enriched are shown. The Netcarto algorithm returned a total of 41 modules for the 660 ORF pairs in dataset A (Supplementary Table S6A). Of these, 71 pairs of ORFs lie within modules (Supplementary Table S11). Node color: pink, mutant genes; all remaining nodes (purple in panels **A**–**C** and **E**) are suppressors. In panel **D**, suppressor nodes are colored according to their known occurrence in various RNA Pol II sub-complexes (yellow: TFIID/SAGA complex; purple, SWI/SNF complex; dark pink, RNA Pol II core complex; light blue, SRB/Mediator complex; green, TFIIE complex; red, TFIIB complex). Edge color: green, genetic interaction (GI); blue, physical interaction, yellow, DS interaction; purple, co-expression; brown, shared protein domains.

Models of dosage suppression

Magtanong *et al.* (33) had shown several mechanisms of dosage suppression, including suppression via direct PPI, suppression by over-expressing gens upstream or downstream of mutant alleles, DSs acting as molecular chaperones and DSs involved in transcription and translation processes acting presumably by readjusting gene expression levels. By examining the collection of DSs found in this study we have noted all previously described mechanisms of suppression. Additionally, the collection of DSs we identified allowed us to probe two facets of underlying genomic plasticity, presumably important for molecular adaptation in evolution: (i) structural plasticity: a high degree of structural robustness of a protein machine (RNA Pol II complex) that can resist mutational impairment of many essential components through alternate interactions, (ii) functional plasticity: functional rewiring of cellular pathways utilizing promiscuous functions of genes (meiotic genes suppressing mitotic impairment of chromosome condensation). These models of suppression are illustrated in Figure 3A–D.

Structural plasticity revealed by dosage suppressors

In a previous genome-wide report, a large proportion of gain-of-function suppressors of missense mutant alleles were found to function through direct protein–protein contact, presumably by stabilizing PPI by mass action. This would imply that most such suppressors should encode proteins known to directly interact with the products of the mutant genes that they suppress—thus, both the mutant protein and its suppressor should be components of the same PPI complex. To test how often genes whose products are known to function within the same macromolecular complex can suppress mutations that affect products within the same or related complexes, we chose as a test bed a well studied protein machine—the RNA polymerase II (RNA Pol II) complex (59). RNA Pol II core (12 subunits) is recruited to the promoter by the general transcription factors TBP, TFIIA and TFIIB (1 subunit each), and TFIIF (3 subunits), with the help of the SRB/mediator complex (25 subunits), to form the pre-initiation complex, following which TFIIE (2 subunits) and TFIIH (9 subunits) are recruited (60). The SWI/SNF (11 subunits) and SAGA (22 subunits) complexes facilitate chromatin remodeling during transcription initiation (59). Extensive GI studies among mediator complex proteins have been reported (61). We scanned eight mutant genes, each of which encoded a defective (or had a complete loss of one) transcription initiation complex protein (62,63), for gene dosage suppression by 75 sub-complex genes (Supplementary Table S12 and Supplementary Figure S6). Six mutants were *ts* lethal due to missense mutation (*med4, med11, tfb3, rad3, kin28, taf12*); two were *ts* deletion mutants (*rpb4Δ* and *taf14Δ*). The deletion mutants had complete deletion of the respective structural genes, such that there was no possibility of expression of any remnant protein fragment (49,64).

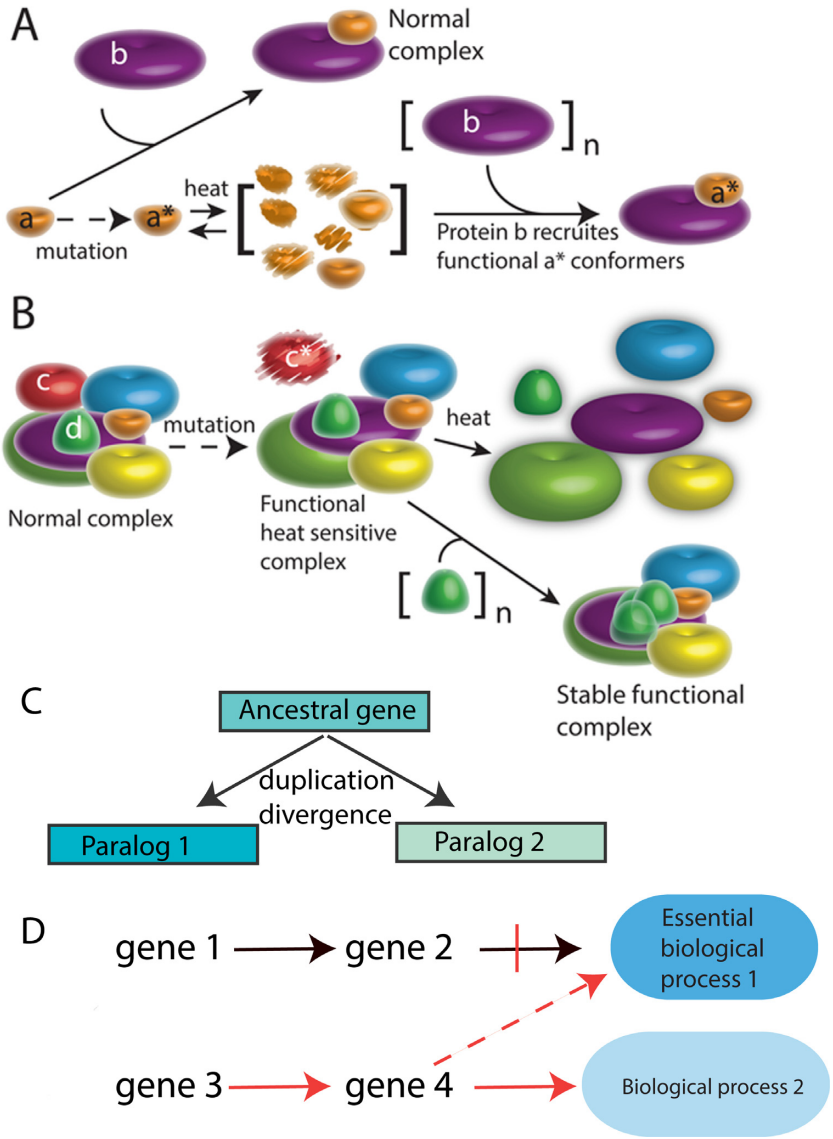

Figure 3. Models of dosage suppression through structural and functional plasticity. (**A**) Suppression of the effects of missense mutation by direct protein–protein interaction (PPI) through mass action. Mutation causes a structural defect in protein **a** to make a heat labile protein **a***, which is destabilized at the restrictive temperature producing a distribution of structural isomers. Misfolded **a*** species are unable to form the functional **a-b** complex. However, if its interaction partner **b** is over-expressed, it recruits the minority fraction of the properly folded isomer, thus pushing the production of the functional **a*-b** complex through mass action. This mechanism of robustness is due to the structural plasticity of individual folding states of proteins. (**B**) Suppression of the effects of mutant alleles by direct PPI. Such genes conceivably encode proteins that are parts of essential protein complexes, but these proteins themselves may not be essential. Their role is to stabilize the macromolecular complex by directly interacting with members of the otherwise heat-labile complex. Missense or deletion mutations in such genes make these complexes heat sensitive. Heat stability is restored by over-expressing another member of these complexes through reinforcing PPIs. (**C**) Suppression by paralogs. An ancestral gene duplicates; the two copies diverge and specialize by mutation, generating two paralogous genes. However, sufficient ancestral function may be retained by both paralogs, such that under abnormal conditions, such as high expression, the latter could suppress a loss of function mutation in the former. Alternatively, both paralogous genes might separately suppress a lethal mutation in a third gene. (**D**) Suppression by rewiring. An essential biological process 1 might be dependent on gene 1 and gene 2. In the event that one of these genes is mutated the organism dies. However, one of genes 3 or 4 might be able to restore viability by an alternate pathway that was specialized for a separate biological process 2, but is artificially recruited (e.g., by abnormal expression in time, developmental phase or intracellular compartment) to rescue a defect in biological process 1.

A total of 31 out of 122 DS-mutant interactions reside within the respective complexes (Figure 4A). For example, *MED11, NUT1, GAL11, ROX3, SRB5* and *SRB7* each suppressed *med4*. By contrast, nearly three times as many mutant-suppressor interaction pairs (91/122 compared to 31/122; $P = 0.0001$ by Fisher's exact test) overlapped two separate sub-complexes (e.g. suppression of *med4* by *TFB3* of TFIIH complex and *RPC10* of Pol II core complex, respectively). Suppressor interactions were specific: e.g. *TFA1* (TFIIE complex) suppressed *med4* but not *med11*—both of the latter encode mediator proteins. Similarly, *SNF11* and *SNF12* of the SWI/SNF complex each suppressed *tfb3* but not *kin28* (TFIIH); *RPO21* (Pol II core) suppressed both *tfb3* and *kin28*. We discovered 36 suppressors of the eight

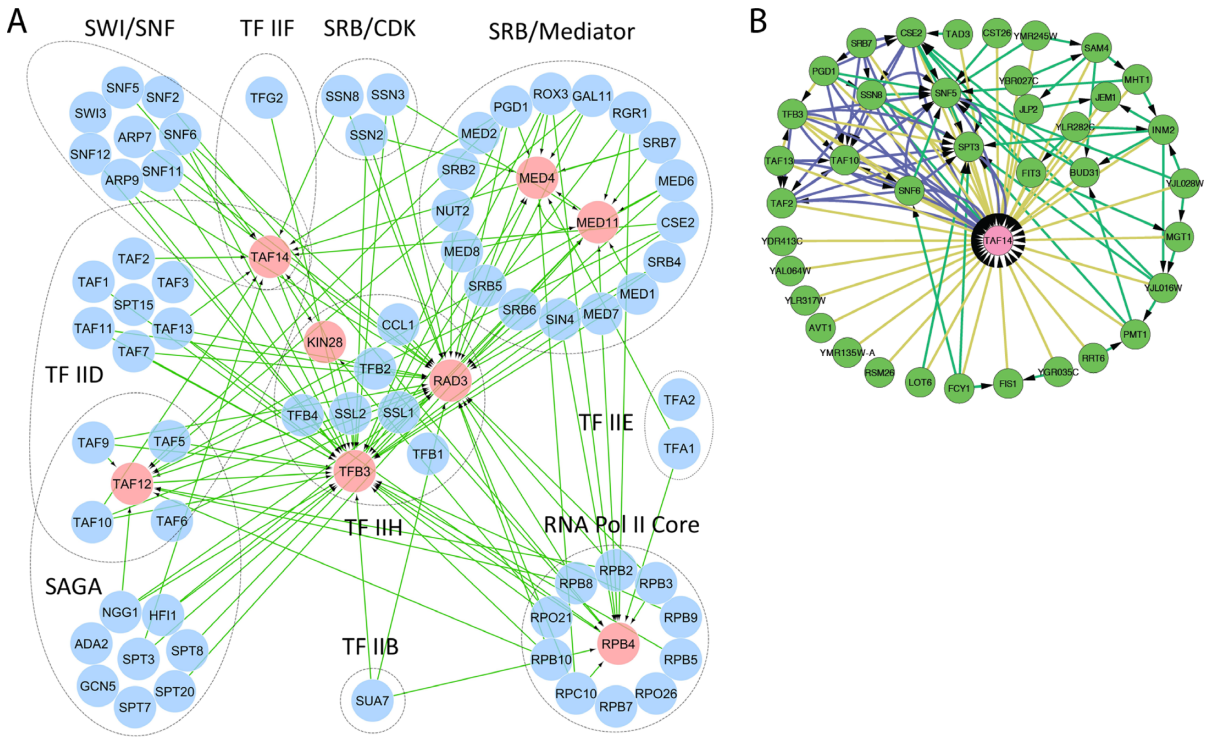

Figure 4. Robustness of RNA Pol II complexes. (**A**) Suppressors of RNA Pol II mutants. We chose eight *ts* mutant genes (RNA Pol II core complex: *rpb4Δ*; mediator complex: *med4* and *med11*; TFIID: *taf12* and *taf14Δ*; TFIIH: *rad3*, *tfb3* and *kin28*) and scanned these for dosage suppression by 75 RNA polymerase II complex genes. DSs (at the base of each arrow) of mutant proteins (at the head of each arrow) are indicated. Node color: pink, proteins encoded by the mutated genes (note: only *taf14* and *rpb4* are deletion mutants, the rest are all missense mutants); blue, suppressor proteins. Note, Taf14p, Med4p and Med11p also suppress other mutations when over-expressed. Not all sub-complex proteins are shown. Edge color: green, dosage suppression, arrow denotes the direction of suppression. Example titration results are in Supplementary Figure S6. (**B**) Co-suppression network of *taf14Δ* as derived from genome wide DS screen. Edge color: yellow, dosage suppression; green, GI; blue, PPI. Some PPI interactions are directed (bait–prey interactions) and some are undirected.

RNA Pol II gene mutations, which are not known to be members of the RNA Pol II complex genes (Supplementary Table S2). The most striking example involves *taf14Δ* (Figure 4B), which yielded 27 suppressors, most of them encoding proteins outside the RNA Pol II complex, 12 of which are genes of unknown function. These results demonstrate the remarkable ability of this essential protein machine to function despite drastic genetic perturbations. It appears that the fragility introduced by the mutant alleles can be overcome by numerous alternate protein–protein contacts.

Functional plasticity by genetic rewiring

The genome wide suppressor dataset allowed us to explore suppression mechanisms quite different from that by direct PPI: we provide examples wherein increased expression of genes allowed the bypass of an essential gene function by engaging *alternate* genetic pathways. Results described below show that the suppression of *smc2* mutation by at least two different suppressor genes appear to proceed through this general mechanism, including the engaging of proteins important for control of meiosis to an otherwise mitotic cellular division cycle.

Smc2p is a DNA-binding subunit of the Smc2p/Smc4p condensin complex (65–67) required for sister chromatid (SC) alignment, separation and inhibiting SC recombination during mitosis (65,68). We identified four strong DSs of *smc2*: *UME1*, *MEK1*, *HTA2* and *SNU66* (Figure 5A). Strikingly, the first two are known to play mutually opposing functions (69–71): *UME1* is a mitotically expressed gene required for the repression of a subset of meiotic genes, including those important for meiotic homologous recombination and *MEK1* is a meiosis specific protein kinase that promotes meiotic homologous recombination by suppressing SC recombination. To provide more insights into the mechanisms of suppression, we analyzed the time course of mRNA expression by these four suppressed *smc2-8* mutant strains at the restrictive temperature (temperature was shifted immediately upon transfer to the medium containing galactose, which corresponded to time '0') and compared their global gene expression patterns with that of the mutant complemented by pGAL:SMC2 (See 'Materials and Methods' section).

Results (Figure 5B and C) show that all four suppressors partially induce the expression of some meiosis-related genes. This led us to propose and test a simple model of *smc2* dosage suppression mechanism, in which meiosis specific genes rescue *smc2* defects in mitosis (Figure 5D and E): *smc2* mutation, which causes a failure of chromosome condensation in mitosis, allows the initiation but not the resolution of SC recombination, thus blocking mitosis (65). Ectopic expression of meiosis-specific genes in the suppressed strains either prevents precocious SC recombination or resolves the SC recombination intermediates allow-

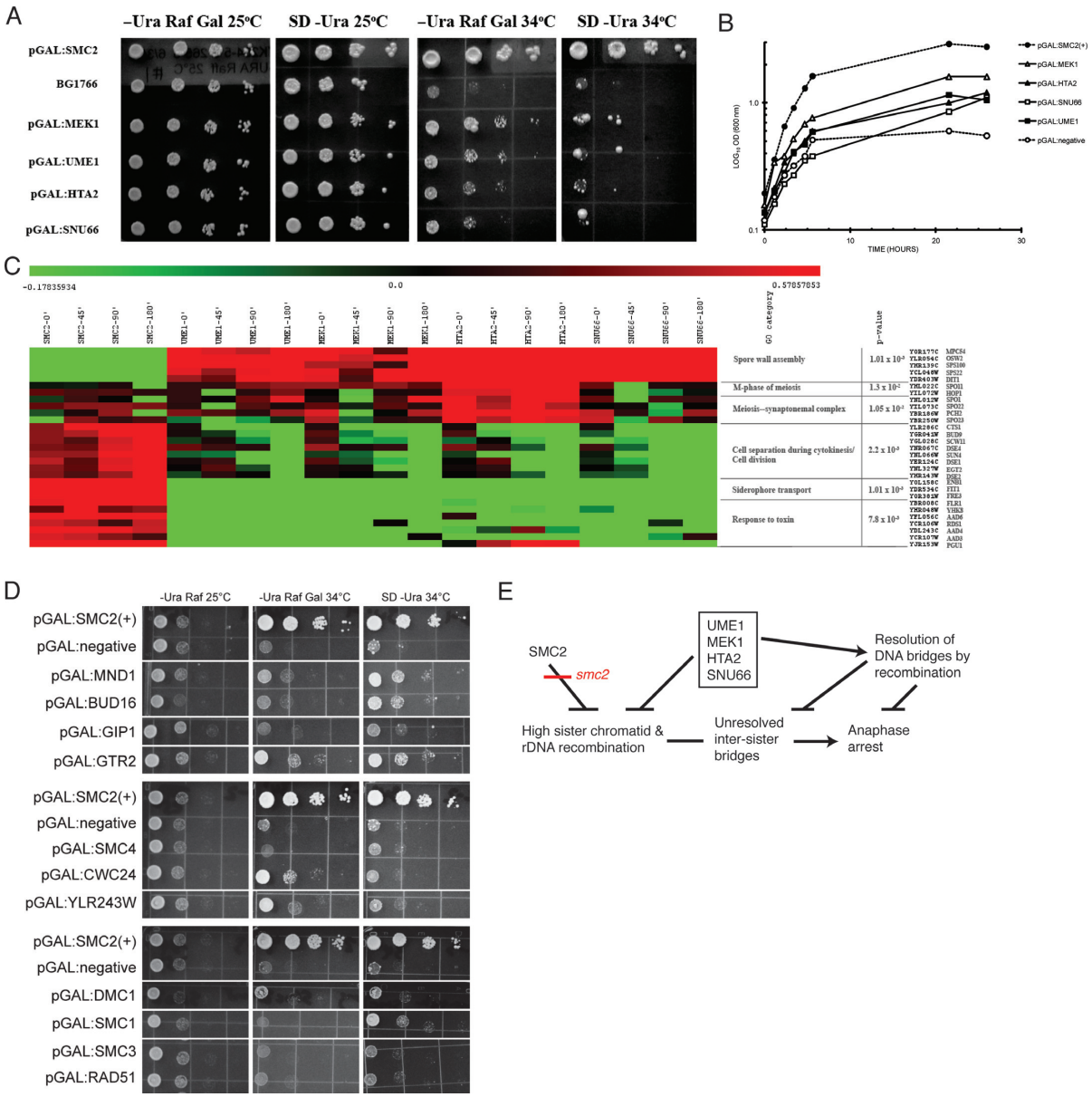

Figure 5. Network rewiring as a mechanism of suppression. (**A**) Cell cycle checkpoint arrest by *smc2-8* at the restrictive temperature is suppressed by galactose-induced expression of *UME1*, *MEK1*, *HTA2* and *SNU66*. (**B**) Growth curves of the suppressed strains. *Smc2-8* strains harboring pGAL:SMC2, pGAL:UME1, pGAL:MEK1, pGAL:HTA2, pGAL:SNU66 and the negative control MORF plasmid (pGAL:negative, BG1766), respectively. Samples taken from these cultures were used in gene expression profiling. (**C**) Heat map of differentially expressed genes. Cell cultures were grown in the presence of galactose at the permissive temperature to early logarithmic phase, then rapidly shifted to the restrictive temperature; 0 time point corresponds to temperature shift. This is described in detail in 'Materials and Methods' section ('RNA methods'). Normalized $\log_2$ transformed mRNA levels of genes were re-normalized against corresponding expression levels in the negative control strain, the resulting expression ratios were filtered for signals above $\pm 2\sigma$ and hierarchically clustered. The first four time points are $\log_2$ ratios of expression values of *smc2-8*/pGAL:SMC2 to that of *smc2-8*/pGAL negative control plasmid. The remaining lanes are $\log_2$ ratios of expression values of *smc2-8*/pGAL:UME1, *smc2-8*/pGAL:MEK1, *smc2-8*/pGAL:HTA2 and *smc2-8*/pGAL:SNU66, respectively, to that of *smc2-8*/pGAL:SMC2. (**D**) Results of a focused screen for additional *smc2-8* suppressors. Only a few suppressors of various strengths are shown. (**E**) Mechanisms of *smc2-8* suppression deduced from the phenotype and suppression network.

ing mitotic division to progress. This model is a particular instance of the general mechanism shown in Figure 3D. Specifically, a non-essential meiotic gene module controlling recombination replaces the essential mitotic gene module controlling chromosome condensation. We tested an implication of this hypothesis by introducing 37 MORF clones (Supplementary Table S13) corresponding to two categories of genes into *smc2-8* and assaying their ability to suppress the *ts* growth defect: (i) other SMC complex genes, and (ii) several meiotic recombination-promoting genes. 29/37 genes so tested suppressed *smc2-8* (examples shown in Figure 5D). Among those that suppressed *smc2-8*, were *RAD51*, *DMC1* and *MND1*—all three are recombination-promoting genes, although *RAD51* was a weak suppressor and all suppressions were galactose-independent. Several intron-containing meiosis-specific recombination genes, in-

cluding *DMC1* and *MND1,* are expressed and spliced to the mature mRNAs at low levels in mitosis but are expressed highly and spliced efficiently in meiosis (72). The function of *DMC1* is to promote recombination between homologous chromosomes and also to inhibit SC exchange in meiosis (73). Dmc1p participates in a cascade of reactions activated through phosphorylation by Mek1p (70), which we have found also to be a suppressor of *smc2*. These results support the idea that at least one mechanism of suppression of *smc2* is through mitotic expression of meiotic recombination genes, which are expected to prevent the formation of or to promote the resolution of sister-chromatid junctions that occur at high frequency in *smc2* mitosis.

DISCUSSION

The collection of 660 DS-mutant pairs discovered in this work supplements 1626 pairs reported previously in the literature (38) and 254 interactions that were discovered in a recent high-throughput experiment (33). The genome wide network of DSs allowed us to explore functional relatedness among the co-suppressors. Mapping of the mutant-suppressor pairs on a PPI network revealed boundaries of topologically defined protein modules. By examining specific protein modules through suppressors of selected RNA Pol II gene mutants, we found that high expression of the genes for specific component proteins within large protein assemblies can functionally replace the absence or the reduction of specific essential components. These latter results underscore the importance of including systematic dosage suppression data in deriving systems-level models of large protein complexes and their pathways of self-assembly.

In principle, dosage-suppressor interactions may involve high affinity and high probability PPIs that enable the system to return to the original state by positive and/or negative feedback effects (buffering interactions). In one scenario, over-produced suppressor products stabilize the corresponding thermo-sensitive missense mutant protein by direct interaction, through recruiting functionally competent folding intermediates from a distribution of folded states. By contrast, suppressors of deletion mutations, such as those of *rpb4Δ* and *taf14Δ*, in which the entire coding frames were deleted, cannot possibly exert their effects by stabilization through direct PPI. Surprisingly, deletion *ts* alleles had a similar average frequency of suppressors (121 interactions with 10 mutants) as did missense *ts* alleles (539 interactions with 43 mutants). This suggests that heat sensitive biological processes (for *ts* deletion mutations) are as suppressible as processes catalyzed by individual heat-sensitive proteins (for *ts* missense mutations). Thus, the suppression mechanisms of *rpb4Δ* by *RPB3* (RNA Pol II core) and by *ROX3* (mediator) likely involve direct or indirect functional replacement of Rpb4p. One mechanism might be the stabilization of the RNA Pol II preinitiation complex by the over-expression of one of the component proteins, such that the preinitiation complex rendered heat labile by *rpb4Δ* is made more robust by an overabundance of Rpb3p or Rox3p. A similar argument holds for the suppression of *taf14Δ* by *TAF2, TAF13* and *TAF10* (all TFIID), *TFB3* (TFIIH), *SRB7, PGD1, CSE2* (all mediator/SRB), *SPT3* (SAGA), and by *SNF5* and SNF6 (both SWI/SNF). Such alternate functional replacements within and between protein complexes reflect a high degree of compositional plasticity, and might also imply alternate pathways of assembly of multi-protein complexes. These observations are generally consistent with the recent observation that RNA Pol II open complexes can be reactivated by the TFIIE complex through stabilizing effects on relatively unstructured domains on mediator proteins (74). Such 'Intrinsically Disordered Regions' serve to functionally assemble RNA pol II complex subunit proteins (64,75) and thus provide a high degree of modular functionality.

Although 43 of 53 suppressed mutant alleles are missense mutations, and several suppressors encode protein folding or processing enzymes such as chaperones or heat shock proteins (*HSC82*, *HSP32* and *CCT6*) or chaperone interacting protein (*MPD1*), there is no significant statistical enrichment for these classes of proteins in the dataset produced in this work. By contrast, there is a significant enrichment for ribosomal proteins in our dataset (B-H corrected $P = 2.64 \times 10^{-4}$) as in the full set of known DSs (B-H corrected $P = 4.5 \times 10^{-6}$). The suppression of *cdc37* (a co-chaperone mutant) by *RPS18A*, *RPL25* and *RPS24B* is consistent with the possibility that some ribosomal proteins may have weak chaperone-like activity (76). Additionally, recent studies indicate that the stoichiometry of ribosomal proteins affects gene expression profiles of specific mRNA populations (77). Thus, at least some of the suppressions involving ribosomal protein genes could possibly involve translational regulation.

Some suppressors of *smc2-8* appear to act through direct PPI with the mutant protein. For example, *SMC1* and *SMC3*, required for SC cohesion, but not the condensin gene *SMC4*, can suppress *smc2-8* (Figure 5D). PPI between the mutant Smc2-8p and Smc1p/Smc3p cohesin complex might be able to stabilize misfolded Smc2-8p, whereas direct interaction between Smc2-8p and Smc4p, both members of the condensing complex, cannot do so. A recent report indicates that Smc2p homolog from *Schizosaccharomyces pombe* interacts with the *S. pombe* histone H2A and H2A.Z proteins in recruiting the condensin proteins to mitotic chromosomes (78). Since *S. cerevisiae HTA2* encodes a homolog of *S. pombe H2A* gene family, it is possible that Hta2p also recruits Smc2p to the nucleosome in an analogous manner. If true, at least a part of the suppression mechanism by *HTA2* might be explained by the stabilization of mutant Smc2p through direct PPI with Hta2p.

Dosage suppression by rewiring, in contrast to that by direct PPI, may involve low affinity and/or low probability interactions that illustrate alternative—redundant or degenerate—pathways. These pathways of suppression appear to decouple physical interaction modules from the modules of functional activities, and the flexible interaction edges rearrange the functional modules to buffer the effects of genetic and environmental perturbations (4,27).

In this work, mechanisms of suppression of a defect in chromosome condensation revealed insights on the potential of unrelated genes that could be brought to bear on solving problems associated with defective cellular processes. It is conceivable that yeasts in nature, and organisms in general, depend on the rewiring of gene regulatory circuits to find new solutions to essential cellular processes during evo-

lution under selective pressure, as observed in this work that meiotic genes relieve mitosis blockage. Such a possibility was investigated earlier in evolved yeast strains with a deletion in an essential gene (*myo1*), where aneuploidy and large-scale variation in the transcriptome were associated with survival (79). While aneuploidy was a recurrent theme observed in that work, it was also estimated that the number of available genetic solutions to a lethal perturbation might be limited. Our finding that nearly six times as many genes can suppress 53 deleterious mutations indicates a high degree of robustness built into the genome, and illustrates potential pathways for rewiring of the genome. It is conceivable that a deleterious mutation in an essential gene, leading to growth arrest, is followed by genomic changes that are often observed in stationary phase cells (79–83); these changes could in principle activate suppressor pathways to restore viability and provide adaptation. The network of DSs of essential gene mutants is analogous to the network of genes that could potentially bypass, if aberrantly expressed, a drug target gene function (e.g. of a cancer-essential gene) for tumor cell survival. Such a network for a cancer cell is the equivalent of potential pathways for developing resistance to cancer chemotherapy, or, analogously, for evolving independence from the checkpoints that ensure non-proliferative growth, which evidently occurs frequently during the development of cancers.

SUPPLEMENTARY DATA

Supplementary Data are available at NAR Online.

ACKNOWLEDGEMENTS

We thank Dr C. Boone (U. Toronto) for discussion, for sharing strains and their suppressor data before publication, B. Kraynack and K. Svay for initial work in suppressor discovery and C. Cordova, R. Vasudevan, V. Padmakumar, K. Bheda, K. Datta, A. Kamra, D. Lev, M. Pollock and S. Russell for technical assistance, and Dr C. Murre (UCSD) for comments on an earlier version of the manuscript.
Author contributions: B.P., Y.K., A.W.S., G.Y. J.P.F., R.R.V., A.H., B.Ø., A.B., B.M. and J.K.T. conducted experiments and analyzed data, A.K. conducted experiments; B.P., Y.K., A.W.S., J.P.F., R.R.V., A.H., B.Ø., A.B., B.M., N.S.B., E.J.G., D.J.G., G.Y., A.Rav., C.A., E.M.P and A.Ray designed experiments and analyzed data; B.P., A.W.S., G.Y., J.P.F., A.H., B.Ø., A.B., D.J.G., A.Rav., C.A. and A.Ray wrote the manuscript; E.J.G., D.J.G., A.Rav., C.A., E.M.P. and A.Ray. procured funding.

FUNDING

National Science Foundation (Frontiers in Integrative Biological Research) [0527023 to D.J.G, E.J.G., E.M.P., C.A., A.Rav., A.Ray.; 0523643 to A.Rav., A.Ray.; 0941078 to A.Ray.]; National Institutes of Health [1R01GM084881-01 to A.Ray.). Funding for open access charge: Internal institutional sources.
Conflict of interest statement. None declared.

REFERENCES

1. El-Samad,H., Kurata,H., Doyle,J.C., Gross,C.A. and Khammash,M. (2005) Surviving heat shock: control strategies for robustness and performance. *Proc. Natl. Acad. Sci. U.S.A.*, **102**, 2736–2741.
2. Kondrashov,A.S. (1994) Sex and deleterious mutation. *Nature*, **369**, 99–100.
3. Gu,Z., Steinmetz,L.M., Gu,X., Scharfe,C., Davis,R.W. and Li,W.H. (2003) Role of duplicate genes in genetic robustness against null mutations. *Nature*, **421**, 63–66.
4. Chen,B.S., Tsai,K.W. and Li,C.W. (2015) Using nonlinear stochastic evolutionary game strategy to model an evolutionary biological network of organ carcinogenesis under a natural selection scheme. *Evol. Bioinform. Online*, **11**, 155–178.
5. Little,J.W., Shepley,D.P. and Wert,D.W. (1999) Robustness of a gene regulatory circuit. *EMBO J.*, **18**, 4299–4307.
6. Nowak,M.A., Boerlijst,M.C., Cooke,J. and Smith,J.M. (1997) Evolution of genetic redundancy. *Nature*, **388**, 167–171.
7. Isalan,M., Lemerle,C., Michalodimitrakis,K., Horn,C., Beltrao,P., Raineri,E., Garriga-Canut,M. and Serrano,L. (2008) Evolvability and hierarchy in rewired bacterial gene networks. *Nature*, **452**, 840–845.
8. Patrick,W.M., Quandt,E.M., Swartzlander,D.B. and Matsumura,I. (2007) Multicopy suppression underpins metabolic evolvability. *Mol. Biol. Evol.*, **24**, 2716–2722.
9. Wagner,G.P. and Altenberg,L. (1996) Complex adaptations and the evolution of evolvability. *Evolution*, **50**, 967–976.
10. Kirschner,M. and Gerhart,J. (1998) Evolvability. *Proc. Natl. Acad. Sci. U.S.A.*, **95**, 8420–8427.
11. Kitano,H. (2004) Biological robustness. *Nat. Rev. Genet.*, **5**, 826–837.
12. Hintze,A. and Adami,C. (2008) Evolution of complex modular biological networks. *PLoS Comput. Biol.*, **4**,e23–e34.
13. Raval,A. and Ray,A. (2013) *Introduction to Biological Networks*. Chapman & Hall/CRC Press, Boca Raton.
14. Hintze,A. and Adami,C. (2010) Modularity and anti-modularity in networks with arbitrary degree distribution. *Biol. Direct*, **5**, 32–57.
15. Siegal,M.L. and Bergman,A. (2002) Waddington's canalization revisited: developmental stability and evolution. *Proc. Natl. Acad. Sci. U.S.A.*, **99**, 10528–10532.
16. Landry,C.R., Lemos,B., Rifkin,S.A., Dickinson,W.J. and Hartl,D.L. (2007) Genetic properties influencing the evolvability of gene expression. *Science*, **317**, 118–121.
17. Becskei,A. and Serrano,L. (2000) Engineering stability in gene networks by autoregulation. *Nature*, **405**, 590–593.
18. Mangan,S., Zaslaver,A. and Alon,U. (2003) The coherent feedforward loop serves as a sign-sensitive delay element in transcription networks. *J. Mol. Biol.*, **334**, 197–204.
19. Mangan,S. and Alon,U. (2003) Structure and function of the feed-forward loop network motif. *Proc. Natl. Acad. Sci. U.S.A.*, **100**, 11980–11985.
20. Fraser,H.B. (2005) Modularity and evolutionary constraint on proteins. *Nat. Genet.*, **37**, 351–352.
21. Ma,W., Lai,L., Ouyang,Q. and Tang,C. (2006) Robustness and modular design of the Drosophila segment polarity network. *Mol. Syst. Biol.*, **2**, 70–79.
22. Kurata,H., El-Samad,H., Iwasaki,R., Ohtake,H., Doyle,J.C., Grigorova,I., Gross,C.A. and Khammash,M. (2006) Module-based analysis of robustness tradeoffs in the heat shock response system. *PLoS Comput. Biol.*, **2**, e59.
23. Ingolia,N.T. (2004) Topology and robustness in the Drosophila segment polarity network. *PLoS Biol.*, **2**, e123.
24. Barabasi,A.L. and Oltvai,Z.N. (2004) Network biology: understanding the cell's functional organization. *Nat. Rev. Genet.*, **5**, 101–113.
25. Jeong,H., Mason,S.P., Barabasi,A.L. and Oltvai,Z.N. (2001) Lethality and centrality in protein networks. *Nature*, **411**, 41–42.
26. Han,J.D., Bertin,N., Hao,T., Goldberg,D.S., Berriz,G.F., Zhang,L.V., Dupuy,D., Walhout,A.J.M., Cusick,M.E., Roth,F.P. *et al.* (2004) Evidence for dynamically organized modularity in the yeast protein-protein interaction network. *Nature*, **430**, 88–93.
27. Chen,B.S. and Ho,S.J. (2014) The stochastic evolutionary game for a population of biological networks under natural selection. *Evol. Bioinform. Online*, **10**, 17–38.
28. Gavin,A.-C., Aloy,P., Grandi,P., Krause,R., Boesche,M., Marzioch,M., Rau,C., Jensen,L.J., Bastuck,S., Dumpelfeld,B. *et al.*

(2006) Proteome survey reveals modularity of the yeast cell machinery. *Nature*, **440**, 631–636.
29. Wagner,G.P., Pavlicev,M. and Cheverud,J.M. (2007) The road to modularity. *Nat. Rev. Genet.*, **8**, 921–931.
30. Komurov,K. and White,M. (2007) Revealing static and dynamic modular architecture of the eukaryotic protein interaction network. *Mol. Syst. Biol.*, **3**, 110–121.
31. Bandyopadhyay,S., Mehta,M., Kuo,D., Sung,M.K., Chuang,R., Jaehnig,E.J., Bodenmiller,B., Licon,K., Copeland,W., Shales,M. *et al.* (2010) Rewiring of genetic networks in response to DNA damage. *Science*, **330**, 1385–1389.
32. Hartman,P.E. and Roth,J.R. (1973) Mechanisms of suppression. *Adv. Genet.*, **17**, 1–105.
33. Magtanong,L., Ho,C.H., Barker,S.L., Jiao,W., Baryshnikova,A., Bahr,S., Smith,A.M., Heisler,L.E., Choy,J.S., Kuzmin,E. *et al.* (2011) Dosage suppression genetic interaction networks enhance functional wiring diagrams of the cell. *Nat. Biotechnol.*, **29**, 505–511.
34. Gelperin,D.M., White,M.A., Wilkinson,M.L., Kon,Y., Kung,L.A., Wise,K.J., Lopez-Hoyo,N., Jiang,L., Piccirillo,S., Yu,H. *et al.* (2005) Biochemical and genetic analysis of the yeast proteome with a movable ORF collection. *Genes Dev.*, **19**, 2816–2826.
35. Li,Z., Vizeacoumar,F.J., Bahr,S., Li,J., Warringer,J., Vizeacoumar,F.S., Min,R., Vandersluis,B., Bellay,J., Devit,M. *et al.* (2011) Systematic exploration of essential yeast gene function with temperature-sensitive mutants. *Nat. Biotechnol.*, **29**, 361–367.
36. Schmitt,M.E., Brown,T.A. and Trumpower,B.L. (1990) A rapid and simple method for preparation of RNA from Saccharomyces cerevisiae. *Nucleic Acids Res.*, **18**, 3091–3092.
37. Irizarry,R.A., Bolstad,B.M., Collin,F., Cope,L.M., Hobbs,B. and Speed,T.P. (2003) Summaries of Affymetrix GeneChip probe level data. *Nucleic Acids Res.*, **31**, e15.
38. Stark,C., Breitkreutz,B.J., Reguly,T., Boucher,L., Breitkreutz,A. and Tyers,M. (2006) BioGRID: a general repository for interaction datasets. *Nucleic Acids Res.*, **34**, D535–D539.
39. Gasch,A.P., Spellman,P.T., Kao,C.M., Carmel-Harel,O., Eisen,M.B., Storz,G., Botstein,D. and Brown,P.O. (2000) Genomic expression programs in the response of yeast cells to environmental changes. *Mol. Biol. Cell*, **11**, 4241–4257.
40. Hughes,T.R., Marton,M.J., Jones,A.R., Roberts,C.J., Stoughton,R., Armour,C.D., Bennett,H.A., Coffey,E., Dai,H., He,Y.D. *et al.* (2000) Functional discovery via a compendium of expression profiles. *Cell*, **102**, 109–126.
41. Pu,S., Wong,J., Turner,B., Cho,E. and Wodak,S.J. (2009) Up-to-date catalogues of yeast protein complexes. *Nucleic Acids Res.*, **37**, 825–831.
42. Kim,W.K. and Marcotte,E.M. (2008) Age-dependent evolution of the yeast protein interaction network suggests a limited role of gene duplication and divergence. *PLoS Comput. Biol.*, **4**, e1000232.
43. Guimera,R. and Nunes Amaral,L.A. (2005) Functional cartography of complex metabolic networks. *Nature*, **433**, 895–900.
44. Enright,A.J., Van Dongen,S. and Ouzounis,C.A. (2002) An efficient algorithm for large-scale detection of protein families. *Nucleic Acids Res.*, **30**, 1575–1584.
45. Byrne,K.P. and Wolfe,K.H. (2005) The yeast gene order browser: combining curated homology and syntenic context reveals gene fate in polyploid species. *Genome Res.*, **15**, 1456–1461.
46. Kellis,M., Birren,B.W. and Lander,E.S. (2004) Proof and evolutionary analysis of ancient genome duplication in the yeast Saccharomyces cerevisiae. *Nature*, **428**, 617–624.
47. Freeman,L.C. (1977) A set of measures of centrality based on betweenness. *Sociometry*, **40**, 440–442.
48. Ruepp,A., Zollner,A., Maier,D., Albermann,K., Hani,J., Mokrejs,M., Tetko,I., Guldener,U., Mannhaupt,G., Munsterkotter,M. *et al.* (2004) The FunCat, a functional annotation scheme for systematic classification of proteins from whole genomes. *Nucleic Acids Res.*, **32**, 5539–5545.
49. Winzeler,E.A., Shoemaker,D.D., Astromoff,A., Liang,H., Anderson,K., Andre,B., Bangham,R., Benito,R., Boeke,J.D., Bussey,H. *et al.* (1999) Functional characterization of the S. cerevisiae genome by gene deletion and parallel analysis. *Science*, **285**, 901–906.
50. Wu,X., Zhu,L., Guo,J., Zhang,D.Y. and Lin,K. (2006) Prediction of yeast protein-protein interaction network: insights from the Gene Ontology and annotations. *Nucleic Acids Res.*, **34**, 2137–2150.
51. Costanzo,M., Baryshnikova,A., Bellay,J., Kim,Y., Spear,E.D., Sevier,C.S., Ding,H., Koh,J.L., Toufighi,K., Mostafavi,S. *et al.* (2010) The genetic landscape of a cell. *Science*, **327**, 425–431.
52. Krogan,N.J., Cagney,G., Yu,H., Zhong,G., Guo,X., Ignatchenko,A., Li,J., Pu,S., Datta,N., Tikuisis,A.P. *et al.* (2006) Global landscape of protein complexes in the yeast Saccharomyces cerevisiae. *Nature*, **440**, 637–643.
53. Yu,H., Braun,P., Yildirim,M.A., Lemmens,I., Venkatesan,K., Sahalie,J., Hirozane-Kishikawa,T., Gebreab,F., Li,N., Simonis,N. *et al.* (2008) High-quality binary protein interaction map of the yeast interactome network. *Science*, **322**, 104–110.
54. Tarassov,K., Messier,V., Landry,C.R., Radinovic,S., Serna Molina,M.M., Shames,I., Malitskaya,Y., Vogel,J., Bussey,H. and Michnick,S.W. (2008) An in vivo map of the yeast protein interactome. *Science*, **320**, 1465–1470.
55. Zhu,J., Zhang,B., Smith,E.N., Drees,B., Brem,R.B., Kruglyak,L., Bumgarner,R.E. and Schadt,E.E. (2008) Integrating large-scale functional genomic data to dissect the complexity of yeast regulatory networks. *Nat. Genet.*, **40**, 854–861.
56. Han,J.D., Bertin,N., Hao,T., Goldberg,D.S., Berriz,G.F., Zhang,L.V., Dupuy,D., Walhout,A.J., Cusick,M.E., Roth,F.P. *et al.* (2004) Evidence for dynamically organized modularity in the yeast protein-protein interaction network. *Nature*, **430**, 88–93.
57. Gunsalus,K.C., Ge,H., Schetter,A.J., Goldberg,D.S., Han,J.D., Hao,T., Berriz,G.F., Bertin,N., Huang,J., Chuang,L.S. *et al.* (2005) Predictive models of molecular machines involved in Caenorhabditis elegans early embryogenesis. *Nature*, **436**, 861–865.
58. Newman,M.E. and Girvan,M. (2004) Finding and evaluating community structure in networks. *Phys. Rev. E Stat. Nonlin. Soft. Matter Phys.*, **69**, 026113–026128.
59. Hampsey,M. (1998) Molecular genetics of the RNA polymerase II general transcriptional machinery. *Microbiol. Mol. Biol. Rev.*, **62**, 465–503.
60. Bushnell,D.A., Westover,K.D., Davis,R.E. and Kornberg,R.D. (2004) Structural basis of transcription: an RNA polymerase II-TFIIB cocrystal at 4.5 Angstroms. *Science*, **303**, 983–988.
61. Collins,S.R., Miller,K.M., Maas,N.L., Roguev,A., Fillingham,J., Chu,C.S., Schuldiner,M., Gebbia,M., Recht,J., Shales,M. *et al.* (2007) Functional dissection of protein complexes involved in yeast chromosome biology using a genetic interaction map. *Nature*, **446**, 806–810.
62. Holstege,F.C., Jennings,E.G., Wyrick,J.J., Lee,T.I., Hengartner,C.J., Green,M.R., Golub,T.R., Lander,E.S. and Young,R.A. (1998) Dissecting the regulatory circuitry of a eukaryotic genome. *Cell*, **95**, 717–728.
63. Woychik,N.A. and Hampsey,M. (2002) The RNA polymerase II machinery: structure illuminates function. *Cell*, **108**, 453–463.
64. Sampath,V., Balakrishnan,B., Verma-Gaur,J., Onesti,S. and Sadhale,P.P. (2008) Unstructured N terminus of the RNA polymerase II subunit Rpb4 contributes to the interaction of Rpb4.Rpb7 subcomplex with the core RNA polymerase II of Saccharomyces cerevisiae. *J. Biol. Chem.*, **283**, 3923–3931.
65. Yu,H.G. and Koshland,D.E. (2003) Meiotic condensin is required for proper chromosome compaction, SC assembly, and resolution of recombination-dependent chromosome linkages. *J. Cell Biol.*, **163**, 937–947.
66. Losada,A. and Hirano,T. (2005) Dynamic molecular linkers of the genome: the first decade of SMC proteins. *Genes Dev.*, **19**, 1269–1287.
67. Huang,C.E., Milutinovich,M. and Koshland,D. (2005) Rings, bracelet or snaps: fashionable alternatives for Smc complexes. *Philos. Trans. R. Soc. Lond. B. Biol. Sci.*, **360**, 537–542.
68. Freeman,L., Aragon-Alcaide,L. and Strunnikov,A. (2000) The condensin complex governs chromosome condensation and mitotic transmission of rDNA. *J. Cell Biol.*, **149**, 811–824.
69. Mallory,M.J. and Strich,R. (2003) Ume1p represses meiotic gene transcription in Saccharomyces cerevisiae through interaction with the histone deacetylase Rpd3p. *J. Biol. Chem.*, **278**, 44727–44734.
70. Niu,H., Li,X., Job,E., Park,C., Moazed,D., Gygi,S.P. and Hollingsworth,N.M. (2007) Mek1 kinase is regulated to suppress double-strand break repair between sister chromatids during budding yeast meiosis. *Mol. Cell. Biol.*, **27**, 5456–5467.
71. Tsukuda,T., Fleming,A.B., Nickoloff,J.A. and Osley,M.A. (2005) Chromatin remodelling at a DNA double-strand break site in Saccharomyces cerevisiae. *Nature*, **438**, 379–383.

72. Juneau,K., Palm,C., Miranda,M. and Davis,R.W. (2007) High-density yeast-tiling array reveals previously undiscovered introns and extensive regulation of meiotic splicing. *Proc. Natl. Acad. Sci. U.S.A.*, **104**, 1522–1527.
73. Schwacha,A. and Kleckner,N. (1997) Interhomolog bias during meiotic recombination: meiotic functions promote a highly differentiated interhomolog-only pathway. *Cell*, **90**, 1123–1135.
74. Cabart,P. and Luse,D.S. (2012) Inactivated RNA polymerase II open complexes can be reactivated with TFIIE. *J. Biol. Chem.*, **287**, 961–967.
75. Toth-Petroczy,A., Oldfield,C.J., Simon,I., Takagi,Y., Dunker,A.K., Uversky,V.N. and Fuxreiter,M. (2008) Malleable machines in transcription regulation: the mediator complex. *PLoS Comput. Biol.*, **4**, e1000243.
76. Kabir,M.A. and Sherman,F. (2008) Overexpressed ribosomal proteins suppress defective chaperonins in Saccharomyces cerevisiae. *FEMS Yeast Res.*, **8**, 1236–1244.
77. Slavov,N., Semrau,S., Airoldi,E., Budnik,B. and van Oudenaarden,A. (2015) Differential Stoichiometry among Core Ribosomal Proteins. *Cell Rep.*, **13**, 865–873.
78. Tada,K., Susumu,H., Sakuno,T. and Watanabe,Y. (2011) Condensin association with histone H2A shapes mitotic chromosomes. *Nature*, **474**, 477–483.
79. Rancati,G., Pavelka,N., Fleharty,B., Noll,A., Trimble,R., Walton,K., Perera,A., Staehling-Hampton,K., Seidel,C.W. and Li,R. (2008) Aneuploidy underlies rapid adaptive evolution of yeast cells deprived of a conserved cytokinesis motor. *Cell*, **135**, 879–893.
80. Argueso,J.L., Westmoreland,J., Mieczkowski,P.A., Gawel,M., Petes,T.D. and Resnick,M.A. (2008) Double-strand breaks associated with repetitive DNA can reshape the genome. *Proc. Natl. Acad. Sci. U.S.A.*, **105**, 11845–11850.
81. Servant,G., Pennetier,C. and Lesage,P. (2008) Remodeling yeast gene transcription by activating the Ty1 long terminal repeat retrotransposon under severe adenine deficiency. *Mol. Cell. Biol.*, **28**, 5543–5554.
82. Naito,K., Zhang,F., Tsukiyama,T., Saito,H., Hancock,C.N., Richardson,A.O., Okumoto,Y., Tanisaka,T. and Wessler,S.R. (2009) Unexpected consequences of a sudden and massive transposon amplification on rice gene expression. *Nature*, **461**, 1130–1134.
83. de Morgan,A., Brodsky,L., Ronin,Y., Nevo,E., Korol,A. and Kashi,Y. Genome-wide analysis of DNA turnover and gene expression in stationary-phase Saccharomyces cerevisiae. *Microbiology*, **156**, 1758–1771.